https://doi.org/10.33271/nvngu/2023-6/048

O. Djezairi[*1],
orcid.org/0009-0007-2829-8186,
A. Bouzidi[2],
orcid.org/0000-0002-4616-6896,
N. Bouzidi[1],
orcid.org/0000-0002-9154-5895,
B. Ayaden[1],
orcid.org/0009-0006-1643-6572,
A. Benselhoub[3],
orcid.org/0000-0001-5891-2860

1 – Laboratory of Materials Technology and Process Engineering (LTMGP), Faculty of Technology, University of Bejaia, Bejaia, Algeria
2 – Electrical Engineering Laboratory (LGE), Faculty of Technology, University of Bejaia, Bejaia, Algeria
3 – Environment, Modeling and Climate Change Division, Environmental Research Center (C.R.E), Annaba, Algeria
* Corresponding author e-mail: omar.djezairi@univ-bejaia.dz

RECYCLING OF BARITE ORE TAILINGS INTO PORCELAIN: MICROSTRUCTURE AND DIELECTRIC PROPERTIES

Purpose. To study the dielectric properties of porcelain obtained from a mixture of sand, kaolin, and feldspar. The latter has been partially substituted with solid barite wastes (SBWs).

Methodology. The study involves preparation of porcelain using conventional solid-state reaction methods, employing two firing temperatures (1200 and 1300 °C) and a soaking time of 3 hours. SBWs are progressively added to the mixtures at levels of 0, 10, 20 and 30 wt%, replacing feldspar content. Structural and dielectric characterizations are conducted to examine the influence of SBWs substitution on macroscopic dielectric properties. Microstructural observations reveal various crystalline phases and micropores, contributing to property effects. Following sintering at 1200 °C, primary mineralogical phases include mullite, anorthite, and quartz. At 1300 °C, the celsian phase emerges alongside anorthite and quartz phases. The technological attributes of the produced porcelain samples, encompassing dilatometric properties, apparent density, and porosity, are determined.

Findings. Dielectric characterization, conducted within the frequency range of 102–105 Hz, demonstrates that the relative constant permittivity values rise from 4.3 to 7.4 for samples sintered at 1200 °C and from 5.1 to 9.9 for those fired at 1300 °C, specifically for samples containing 10 wt% SBWs. Additionally, the dielectric loss tangent decreases with increasing sintering temperature. The macroscopic permittivity of porcelains can be accurately calculated using a mixing rule, which aligns well with experimental results.

Originality. The original contribution lies in the use of 10 wt% Solid Barite Wastes (SBWs) from the Boucaid mine in order to effectively create environmentally friendly porcelain insulators. The study showcases the potential of SBWs as a partial substitute, thus promoting sustainability in porcelain insulator production.

Practical value. The results of this study hold practical significance for the ceramics and insulator manufacturing industries by providing insights into enhancing the dielectric properties of porcelain through the incorporation of SBWs. This approach contributes to the production of environmentally friendly insulators.

Keywords: *concentration tailings, Boucaid mine, barite rejects, microstructure, dielectric properties*

Introduction. The mining industry is one of the pillars of the economic recovery of countries. However, it also poses significant environmental challenges due to the substantial production of residues and waste in various forms, thereby endangering biodiversity [1]. This issue becomes particularly concerning when it involves the enrichment of substances with multiple metallic elements such as galena, sphalerite, barite, etc. This is the case in many mines in Algeria, notably the Boucaid mine. The leaching of sulfur-bearing waste deposits is the result of the combined action of water and wind, which accelerates the environmental degradation process [2]. The oxidation reactions within mining waste deposits rich in sulfide minerals trigger acute acid mine drainage, which harms the environmental quality for wildlife, flora, and water resources [3] due to the process of acid mine drainage resulting from the chemical alteration of these minerals when they come into contact with water. According to the study conducted by [4], it was observed that the concentrations of dissolved oxygen in the water were significantly low, below 5.0 mg/l, while the pH was acidic. Following the studies conducted by [5], it has been found that mining waste from abandoned barite mines leads to water contamination with very high concentrations of heavy metals such as arsenic, barium, iron, mercury, manganese, nickel, lead, and zinc. The studies carried out by [3, 6], on the pollution assessment of the mining region of Ain Azel, and the region of Boucaid showed that the enrichment of polymetallic ore is the potential source of soil contamination by heavy metals, whose concentrations of metals in the sediments were high: 94.79 of Pb, 89.79 of Zn, 21.73 of Cu, 21.46 of Cr, 3.25 of Cd and 44190 of Fe (mg/kg).

Barite-based ceramics ($BaSO_4$) have broad industrial applications, especially in electronic and medical fields, due to their exceptional characteristics such as a low thermal expansion coefficient, high melting points, and a low dielectric constant. Barite ($BaSO_4$) is known for its use as fluxing agents in the production of enamels and ceramic materials [7]. Due to their shielding and protective capacity against X-rays and gamma rays [8], these materials are used in the construction industry,

being effective materials for protecting humans against this type of ionizing radiation [9]. The refractive index of optical glass is enhanced by the addition of barium, which promotes the sintering process and reduces the viscosity of molten glass [10]. Recently, ceramics have been developed using a combination of barite and kaolin derivatives, creating an ideal medium for protecting walls in diagnostic radiology during X-ray exposures [9].

Electrical ceramics have many applications depending on its dielectric properties. Indeed, ceramic materials with dielectric constant above 12 are generally used in capacitors and transducers materials. Besides, dielectric properties of hexacelsian are suitable for substrate materials for semiconductor packaging or multilayered ceramics substrate for high-frequency electric circuits [11]. The ceramic capacitors are some of the most widely used discrete electronic components that play a very important role in electronic industries [7]. Several materials with good microwave dielectric properties have recently been developed for microwave applications, such as resonators, filters and substrates [7, 12]. Recent developments in the separation process enhance the opportunities to stabilize the particle size distribution of used materials [13].

The present work aims to study the application of SBWs as a raw material in the production of porcelain-type ceramics. Feldspar is substituted by SWBs material by 0, 10, 20, 30 wt%; the samples are labeled PCRB0, PCRB10, PCRB20, and PCRB30 respectively. The ceramic samples were sintered at 1200 and 1300 °C during 3 hours' period. Microstructures, physical, and dielectric properties were studied. Furthermore, the evaluation of the release of different chemical species such as lead (Pb^{2+}), zinc (Zn^{2+}), barium (Ba^{2+}), and copper (Cu^{2+}) present in the porcelain samples was examined.

Materials and methods. The prepared reference sample called PCRB0 is composed by kaolin, sand and feldspar with 50, 20 and 30 wt% respectively. Feldspar is substituted by different amounts of SBWs (10, 20 and 30 % wt%), resulting in four distinct mixtures designated as PCRB10, PCRB20, and PCRB30, respectively. All these mixtures were carefully ground for 2 hours in a Fritsch planetary mill using alumina agate balls as the grinding media. The ground product was then dried for 24 hours at 105 °C. Next, the mixture was sieved through a 63 μm sieve, and the resulting powders were pressed at 55 MPa for 10 minutes to obtain pellets, without the addition of a binder, to form pellets with a diameter of 30 mm and a thickness of 4 mm. A portion of the pellets was subjected to calcination at 1200 °C, while another portion was heated to 1300 °C in an electric furnace for 3 hours, with a heating rate of 10 °C/min. In order to determine the chemical composition of the raw material, X-ray fluorescence technique (PanAnalytical Perl'X3 system) was used. Mineralogical analysis was performed using a Bruker D2 Phaser X-ray diffractometer, utilizing CuKα radiation, a step size of 0.02 degrees 2θ, and a counting time of 10 s per step. Quantitative analysis of the different phases present was made from XRD diagrams by Rietveld refinement, using NaF as internal standard. The peak height ratio of mullite {121}, quartz {112}, cristobalite {101}, anorthite {004}, rutile {110} and NaF {200-202} gave the quantity of each phase. The mass percentages of the amorphous phase are determined after knowing the total quantity of the crystalline phases.

The total porosity of the samples was assessed using both absolute and apparent densities. Absolute density was measured using helium pycnometry, while apparent density was obtained through the Archimedes' method using water. The thermal characteristics of each sample were evaluated using dilatometric analysis conducted with a BAHR dilatometer (DIL801L model, Thermoanalyse Gmbh, Hüllhorst, Germany). The capacitance measurements (relative permittivity ε_r; resistivity *R* and dielectric loss tanδ were performed at 25 °C within the frequency range of 102 to 105 Hz using an HP 4284 LCR meter (Hewlett-Packard Japan); both sides of samples were polished and coated with a conductive silver paste.

To assess the environmental impact, the mobility of pollutants was determined by employing the Toxicity Characteristic Leaching Procedure (TCLP) as described by the Environmental Protection Agency (EPA) in its Method 1311:1992. The concentrations in the filtrate were measured using an Inductively Coupled Plasma-Atomic Emission Spectrometer (ICP-AES Agilent 7500).

Results and discussions. ***Chemical and mineralogical compositions of the raw materials.*** As indicated in Table 1, kaolin, sand, and feldspar, contain relatively high amounts of SiO_2 and Al_2O_3, which are 42.40, 95.21, 74.6, and 37.8 wt%, 0.97, 12.9 wt%, respectively. However, flux agents such as Na_2O and K_2O are present in feldspar with 3.7 and 4.6 wt% respectively. Kaolin has a relatively high proportion of TiO_2, accounting for 1.99 wt%. On the other hand, SBWs contain high amount of BaO (20.66 wt%) and CaO (13.00 wt%) as well as metal oxides such as PbO (14.49 wt%). SBWs show a slight amount of Al_2O_3 (1.70 wt%) and relatively high amount of transition metals Fe_2O_3 (6.55 wt%), ZnO (17.99 wt%) and TiO_2 (3.71 wt%). These metal oxides could act as flux agents and play same role as feldspar.

The main crystalline phases constituting the SBWs (Fig.1) are calcite, barite, and quartz. However, the mineralogical composition reveals that the SBWs are primarily composed of barite (25 %), calcite (22 %), cerussite (13 %), quartz (4 %), and hemimorphite (27 %).

Table 1

Chemical composition of the materials used

Oxides	Kaolin (%)	Sand (%)	Feldspar	SBWs
SiO_2	42.40	95.21	74.60	8.61
Al_2O_3	37.80	0.97	12.90	1.70
Fe_2O_3	0.55	0.23	1.73	6.55
MnO	0.07	–	0.04	0.09
MgO	0.05	0.01	0.40	0.91
CaO	0.26	1.32	1.08	13.00
Na_2O	0.03	0.27	3.70	0.07
K_2O	0.02	0.40	4.60	0.30
TiO_2	1.99	0.01	0.30	3.71
P_2O_5	0.01	–	0.03	0.01
ZnO	–	–	–	17.99
BaO	–	–	–	20.66
PbO	–	–	–	14.49
CuO	–	–	–	0.01
L.O. I	16.78	1.58	0.71	11.88

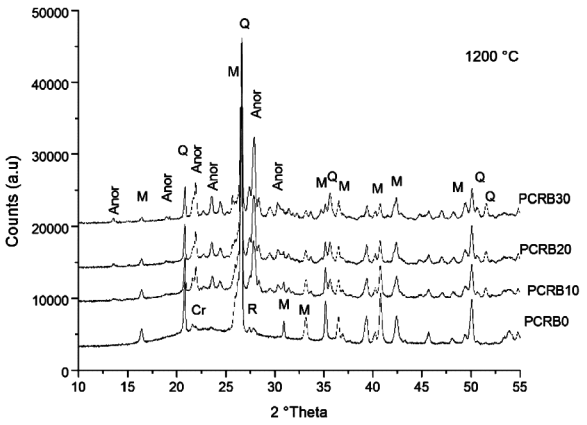

Fig. 1. XRD patterns of SBWs waste

Mineralogical analysis of the sintered samples. The main mineralogical phases observed in Figs. 2, *a* and *b*, corresponding to the samples sintered at 1200 and 1300 °C, respectively, are mullite, anorthite, quartz, and rutile. It is observed that the peaks of quartz and mullite decrease with the addition of SBWs. This can be attributed to the fact that quartz participates in the formation of a glassy phase, which is induced by the presence of fluxing agents in the SBWs [14]. On the other hand, the peaks of anorthite start to increase with the addition of 10 % by weight of SBWs, while the peaks of cristobalite tend to gradually disappear with the increasing amount of SBWs.

The behavior of the samples sintered at 1200 °C (Fig. 2, *a*) differs from that observed when the firing temperature was kept at 1300 °C. With the increase in the amount of SBWs, the peaks intensity corresponding to mullite and quartz decreased. This can be attributed to the transformation of silica into a vitreous phase, likely facilitated by the presence of fluxing agents such as Fe_2O_3, TiO_2, PbO, and ZnO, which play a role in modifying the network structure [14]. On the other hand, the appearance of the anorthite phase ($CaAl_2Si_2O_8$) is attributed to the excessive amount of CaO present in the SBWs (13.00 wt%); this phase increases as the amount of the reject is increased in the ceramic mixtures.

Additionally, a new phase corresponding to the formation of celsian crystals ($BaAl_2Si_2O_8$) was observed in the PCRB30 sample, within the (SiO_2-Al_2O_3-BaO) triaxial composition region. Celsian can form in the high silica region [15]. At the same temperature, the rutile phase disappeared as the amount of SBWs increased, likely indicating its incorporation into the mullite phase [16].

Table 2 presents the quantitative mineralogical analysis of the phases formed during the sintering process of various porcelains. It is seen that the addition of SBWs is accompanied by the increase in glassy phase and formation of anorthite amounts and the decrease in mullite quartz and cristobalite phases. The amount of rutile is much higher in PCRB0 at 1200 °C than in PCRB10 at 1300 °C. However, this phase disappeared when 10 wt% of SBWs was added in the mixture which is probably embedded in the glassy phase or introduced in the mullite structure [16].

Dilatometric behavior of the ceramic mixtures. Fig. 3 shows linear shrinkage of the samples as function of temperature (30–1200 °C). Three-stage sintering process, excluding initial stage, characterized by the mass gain and irreversible moisture expansion of the ceramic bodies as a consequence of its rehydroxylation up to 500 °C were obtained. The first linear shrinkage between (0.5–0.9 %) occurs at 590 °C due to the transformation of $\alpha \rightarrow \beta$ quartz and transformation of kaolin to give metakaolinite phase. A second shrinkage (0.7–1.1 %) occurs at around 940 °C for the samples PCRB0 and PCRB10 to the reorganization of metakaolin to spinel-type and mullite structure and the release of carbonates and sulfur belonging to the barite waste. However, these transformations occur to PCRB30 and PCRB20 at 960 °C with a linear shrinkage of 0.6–0.9 % respectively. The third linear shrinkage (1.7–2 %) occurs at around 1000–1100 °C; increasing with the amount of barite waste in the mixtures. The last linear shrinkage (3.5–5 %) occurs from 1100 °C, attributed to the formation of new crystalline phases as cristobalite, anorthite and celsian. Linear shrinkage of PCRB30 (30 wt% of barite waste) tends to decrease rapidly at around 1180 °C, whereas the linear shrinkage of the other samples continues to decrease.

Porosity of the sintered samples. The porosity measured in relation to the temperature, as presented in Fig. 4, indicates a significant reduction corresponding to the samples fired at 1300 °C. Hence, porcelain without SBWs additions exhibit total porosity of 10 and 3.59 vol% whereas with the addition of 10 wt% of SBWs in the mixtures, porosity of the samples tends to diminish slightly to 9.35 and 2.66 vol% at 1200 and 1300 °C respectively. Then, it increases highly to attain 19.60 vol% at 1200 °C, when 30 wt% of SBWs were added. In opposite, at 1300 °C, porosity of the samples is not excessive, it increased slightly to attain 5.31 vol%. At 1200 °C, with SBWs addition, the obtained porcelains fired at 1200 °C are obviously more porous. This is probably due to the formation of anorthite and quartz crystalline phases beside less of liquid phase formation and poor consolidation of the material during sintering. In this context, excessive content of $BaSO_4$ (>10 wt%) does not make a difference as fluxing agent in the mixtures. Additionally, it

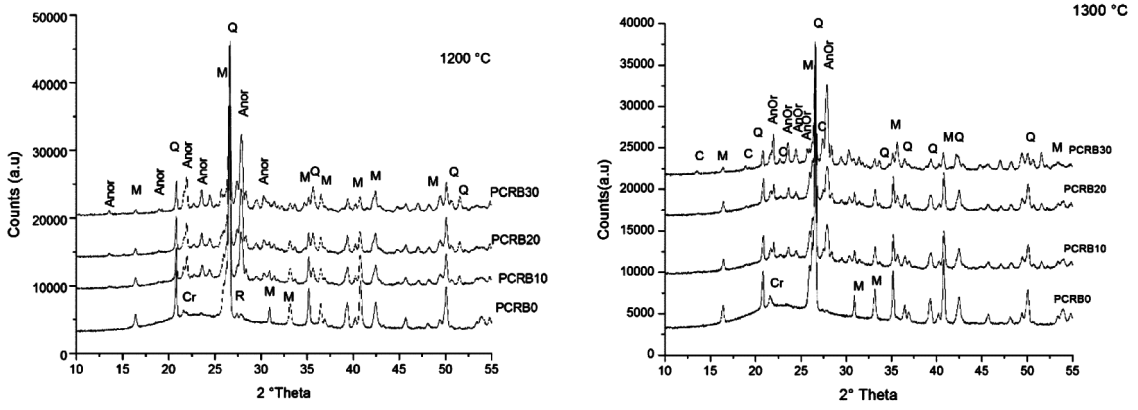

a *b*

Fig. 2. XRD patterns of the ceramic samples fired:
a – at 1200; b – at 1300 °C (M: Mullite; Q: Quartz; R: Rutile; Anor: Anorthite; Cr: Cristobalite; C: Celsian)

Table 2

Quantitative mineralogical analysis of PCRB0 and PCRB10 porcelain

T(°C)	Porcelain	Mullite (%)	Quartz (%)	Cristobalite (%)	Anorthite (%)	Rutile (%)	Glassy phase (%)
1200	PCRB0	18 ± 1	18 ± 2	8 ± 1	0	4 ± 0.5	52 ± 1
	PCRB10	8 ± 0.5	14 ± 1	2 ± 0.5	19 ± 0.5	0	57 ± 0.5
1300	PCRB0	20 ± 0.5	10 ± 1	10 ± 1	0	2 ± 0.5	58 ± 1
	PCRB10	10 ± 1	11 ± 1	4 ± 1	13 ± 0.5	0	63 ± 1

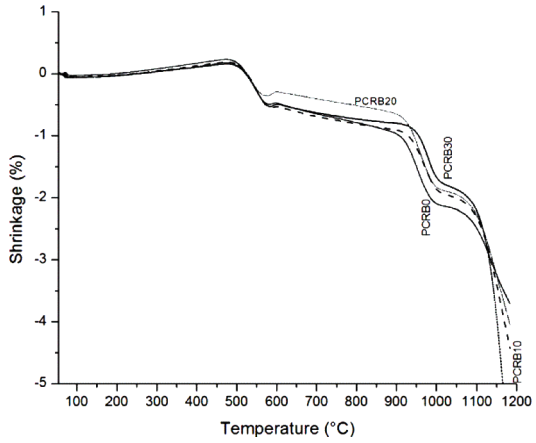

Fig. 3. Dilatometric behavior of the porcelain mixtures as function of temperature

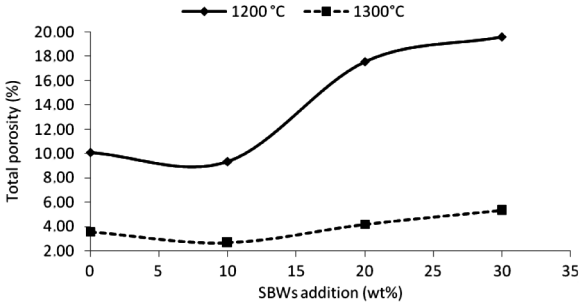

Fig. 4. Total porosity of the samples fired at 1200 and 1300 °C

was shown by Bouzidi [11] that sintering temperature of 1200 °C is insufficient to form spar which might promote growth of the amorphous phase.

Due to the significance of porosity, the firing process cannot be efficiently completed. This can be explained by the fact that the increase in closed porosity begins before the significant reduction in open porosity [17]. The crystallization of mullite and the dissolution of quartz in the liquid phase are the causes of this phenomenon, thereby contributing to an increase in the density of the liquid phase accompanied by a reduction in porosity. The relatively high quantity of BaO (20.66 wt%) induces a more refractoriness behavior during firing at the temperature of 1300 °C, which seems to be too low to promote the formation of the glassy phase. Its leading role in microstructure formation is therefore not completed as for the decrease in porosity [11].

Microstructure of the ceramic samples. The microstructure of the samples with different Barite Solide waste additions was observed by SEM (Fig. 5).

As shown on PCRB0 sample (Fig. 5, *a*) sintered at 1200 °C (without addition of SBWs), microstructure is homogenous and the sample presents open and closed porosities surrounded by a glassy phase. Microstructure of PCRB10 sample (Fig. 5, *b*) (10 wt% of SBWs) sintered at 1200 °C shows closed and open porosities distributed on the surface. As the sintered temperature rises to 1300 °C, microstructure of PCRB10 (Fig. 5, *c*) shows an evident consolidation and densification behavior. Thus, grains of mullite surrounded by vitreous phase were evidenced. Moreover, as the SBWs was added, the sample became heterogeneous showing nano-sized grains of quartz that were not yet melted in the matrix due to the insufficient firing. This can be attributed to the crystallization of glass, resulting from the uneven distribution of Ba^{2+} in the glassy phase during sintering, as reported by Purohit [18].

Dielectric properties of the ceramic samples. The dielectric properties of the samples have been studied as a function of frequency. In this study, the dielectric properties of the samples PCRB20 and PCRB30 were not studied because of their excessive porosity (~19 %). The relative dielectric constant of the samples, sintered at 1200 and 1300 °C with a holding time of 3 hours, as function of frequency are shown in Figs. 6, *a* and *b*). The relative dielectric constant decreased with frequency. This is due to space charge polarization, which was unable to respond quickly to the changing electric field within this frequency range. As a result, orientation polarization played a significant role in the polarization of the ceramic samples [19].

On the one hand, at an intermediate frequency of 100 Hz, relative dielectric constant of the samples sintered at 1200 and 1300 °C (without SWBs addition) are similar as common porcelain values (<6) for both samples which are 4.9 and 5.2, respectively. Thereafter, this parameter increased as function of SWBs contents and sintering temperature. The samples PCRB10 sintered at 1200 and 1300 °C exhibit maximum values of relative dielectric constant 7.46 and 9.0, respectively. This is related to the dissolution of rutile in the glassy phase and possibly to the limited substitution of Al^{3+} by Ti^{4+} in the octahedral sites of mullite, although this has a limited impact on the overall dielectric properties. Besides, the dependence of the dielectric properties, when 10 wt% of SWBs were added, exhibits the same tend as porosity and the glassy phase contents which vary from 9.35 to 2.66 vol% and from 57 to 63 wt% at 1200 and 1300 °C respectively. The macroscopic permittivity of the samples PCRB10 fired at 1200 and 1300 °C were influenced by their microstructural characteristics. Indeed, the increase in cristobalite, secondary mullite and glass contents increases the permittivity of the samples.

It is well known that dielectric constant is related to the ionic polarisability, the unit-cell volume and porosity [18]. Therefore, the frequency dependence of the dielectric properties of the material is influenced by the dipole relaxation associated with impurities and the domain wall motion of the ionic particles [20].

Dielectric losses of porcelains in the frequency range of 102–105 Hz are shown in Figs. 7, *a* and *b*. They are larger at low frequencies than at high frequency. The dielectric loss increases with increase in SWBs content for both sintering temperatures but kept $< 3 \cdot 10^{-2}$. However, as in the case of relative

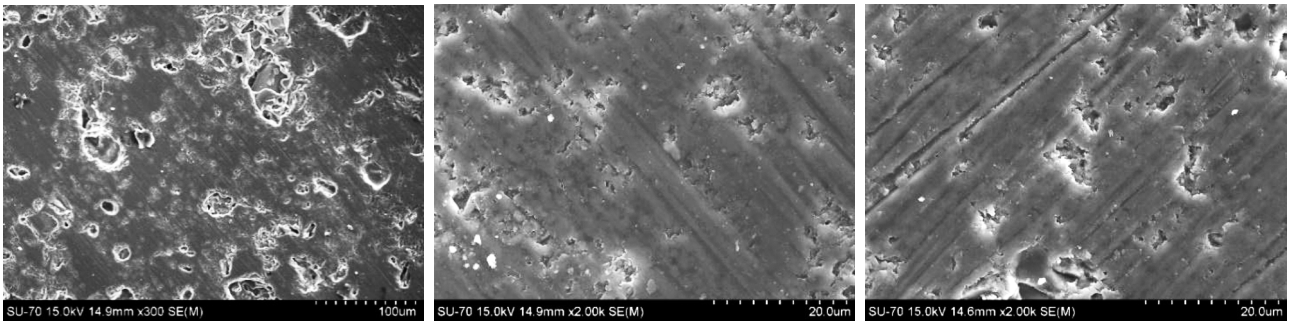

a *b* *c*

Fig. 5. SEM images of the polished surface of the porcelain samples:
a – PCRB0; b – PCRB10 fired at 1200 °C; c – PCRB10 fired at 1300 °C

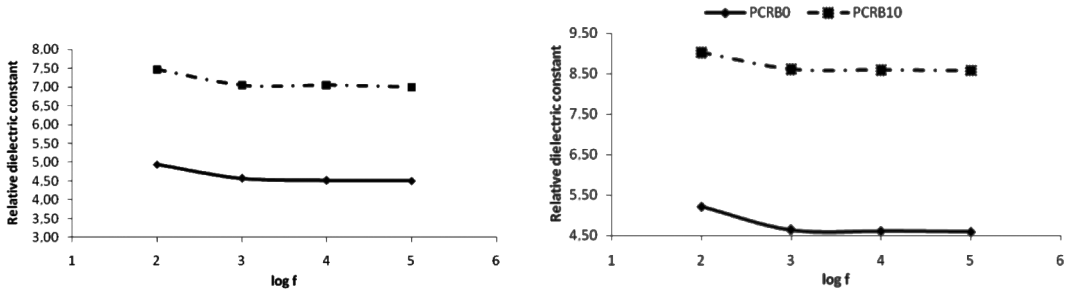

Fig. 6. Relative dielectric constant of the samples as a function of frequency of PCRB0 and PCRB10 sintered at: a – 1200; b – 1300 °C

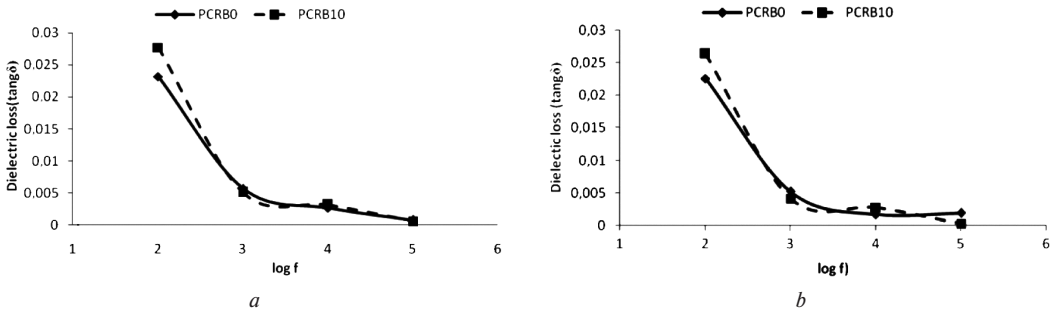

Fig. 7. Dielectric losses of the samples as a function of frequency of PCRB0 and PCRB10 sintered at: a – 1200; b – 1300 °C

dielectric properties, dielectric losses decrease with increase in frequency for both sintering temperatures. This phenomenon is influenced by various factors, including densification, concentration, size distribution, and the morphology of crystalline phases within the glassy matrix [21]. However, porosity (open and closed porosity) plays a negative role, since they exhibit a significant relaxation process at low frequency. Besides this, the boundaries between the crystalline phases are considered the paths that allow dissipation of current from the samples.

Environmental study of the samples. In order to evaluate the degree of metal immobilization, leaching tests were conducted on the ceramic sample PCRB10 (Table 3), which was calcined at temperatures of 1200 and 1300 °C respectively. The samples were ground and subjected to the TCLP method (192). The leachate concentrations were compared to the limits set by the U.S. Environmental Protection Agency (USEPA). According to Table 3, the leachate concentrations of the samples fired at 1200 °C are higher than those of the samples fired at 1300 °C. This can be attributed to the vitrification process of heavy metals, where they are trapped within the glass structure of the ceramic matrix. However, the values were in compliance with the TCLP limits regulated by USEPA, indicating that the leaching test demonstrated a successful immobilization of the heavy metals. This suggests that the addition of 10 wt% of the SBWs to ceramic products is an effective method for inertization.

Table 3

Results of USEPA TCLP tests for PCRB10 after firing at 1200 and 1300 °C, along with the maximum values of contaminants compliant with toxicity characteristics

Components (ppm)	1200 °C	1300 °C	Limits US-EPA (ppm)
Ba	1.053	0.456	100
Pb	0.088	0.054	5
Zn	0.071	0.030	300
Cu	0.047	0.012	5

Conclusions. Due to their mineralogical and chemical composition, barite tailings (SBWs) can be used as raw materials for porcelain production. However, it is important to note that these tailings contain heavy metals that can have adverse effects on the environment due to their chemical composition.

During the sintering process, the intensities of quartz and mullite phases in the ceramic samples decreased, giving way to the formation of the anorthite phase, facilitated by the presence of calcite from the solid barite wastes (SBWs). Additionally, the presence of fluxing agents such as Fe_2O_3, PbO, and ZnO in the SBWs material positively contributes to the promotion of glassy phase formation. It is worth noting that the celsian phase ($BaO\text{-}Al_2O_3\text{-}2SiO_2$) is only present in the PCRB30 sample fired at 1300 °C.

The addition of up to 10 wt% of SBWs resulted in an increase of permittivity since the glassy phase is increased besides the diminution of porosity. However, the anorthite phase plays a positive role to increase the relative permittivity and promotes the formation of glassy phase. Solid Barite Wastes (SBWs) can be recycled by incorporating them at 10 wt% and using them as raw material for the production of environmentally friendly ceramic materials, such as porcelain insulators. This approach offers a potential alternative and reliable solution for the disposal of these wastes, thereby contributing to the preservation of the environment.

Acknowledgements. *We would like to convey our sincere appreciation to everyone, both individuals and organizations, who have played a role in making this research article possible. Our special thanks go to the Center for Scientific and Technical Research in Physico-Chemical Analysis (CRAPC) and to all the individuals at ENOF (National Enterprise for Non-Ferrous Mineral Products and Useful Substances), Boucaid Unit. Their outstanding collaboration during the sample collection phase and their invaluable support are greatly acknowledged.*

References.

1. Bouabdallah, S., Chaib, A., Bounouala, M., Dovbash, N., Benselhoub, A., & Bellucci, S. (2023). Recycling of siliceous by-products to reduce their impacts on the environment. *Technology audit and production reserves*, *2*(3(70)). https://doi.org/10.15587/2706-5448.2023.277784.

2. Bakke, T., Klungsøyr, J., & Sanni, S. (2013). Environmental impacts of produced water and drilling waste discharges from the Norwegian offshore petroleum industry. *Marine Environmental Research, 92*, 154-169. https://doi.org/10.1016/j.marenvres.2013.09.012.
3. Khemmoudj, K., Merabet, S., Bendadouche, H., Bouzaza, A. B., & Balla, E. L. H. (2017). Assessment of Heavy Metal pollution due to the Lead –Zinc Mine at the Ain Azel area (northeast of Algeria). *Journal of environmental research and management, 8*, 001-011. https://doi.org/10.18685/EJERM(8)1_EJERM-16-019.
4. Adamu, C. I., Nganje, T. N., & Edet, A. (2015). Heavy metal contamination and health risk assessment associated with abandoned barite mines in Cross River State, southeastern Nigeria. *Environmental Nanotechnology, Monitoring and Management, 3*, 10-21. https://doi.org/10.1016/j.enmm.2014.11.001.
5. Grigorova, I., Dzhamyarov, S., & Nishkov, I. (2015). Barite flotation concentrates from Kremikovtzi "Black" tailings. *Journal of International Scientific Publications, Materials, Methods and Technologies, 9*, 561-577. https://doi.org/10.18685/EJERM(8)1_EJERM-16-019.
6. Attoucheik, L., Jordanova, N., Bayou, B., Lagroix, F., Jordanova, D., Maouche, S., ..., & Boutaleb, A. (2017). Soil metal pollution from former Zn–Pb mining assessed by geochemical and magnetic investigations: case study of the Bou Caid area (Tissemsilt, Algeria). *Environmental Earth Sciences, 76*, 298. https://doi.org/10.1007/s12665-017-6622-9.
7. Pan, M. J., & Randall, C. A. (2010). A brief introduction to ceramic capacitors. *IEEE electrical insulation magazine*, *26*(3), 44-50. https://doi.org/10.1109/MEI.2010.5482787.
8. Ripin, A., Faizal, M., & Mohd-Idzat, I. (2018). Synthesis of anti-radiation ceramic from raw Malaysian kaolin and barite. *AIP Conference Proceedings, 2030*, 020311. https://doi.org/10.1063/1.5066952.
9. Ripin, A., Faizal, M., Choo, T. F., Yusof, M. R., Hashim, S., & Ghoshal, D. S. (2018). X-ray shielding behaviour of kaolin derived mullite-barites ceramic. *Radiation Physics and Chemistry, 144*, 63-68. https://doi.org/10.1016/j.radphyschem.2017.11.014.
10. Mhareb, M. H. A., Alqahtani, M., Alshahri, F., Alajerami, Y. S. M., Saleh, N., Alonizan, N., & Morsy, M. A. (2020). The impact of barium oxide on physical, structural, optical, and shielding features of sodium zinc borate glass. *Journal of Non-Crystalline Solids*, *541*, 120090. https://doi.org/10.1016/j.jnoncrysol.2020.120090.
11. Bouzidi, N., Bouzidi, A., Nunes, R. O., & Merabet, D. (2018). Study of the microstructure and mechanical properties of halloysite–kaolinite/$BaCO_3$ ceramic composites. *Clay Minerals, 53*, 403-412. https://doi.org/10.1180/clm.2018.29.
12. Huang, L., Ding, S., Yan, X., Song, T., & Zhang, Y. (2020). Structure and microwave dielectric properties of $BaAl_2Si_2O_8$ ceramic with Li_2O–B_2O_3 sintering additive. *Journal of Alloys and Compounds, 820*, 153100. https://doi.org/10.1016/j.jallcom.2019.153100.
13. Beshta, O. S., Kuvaiev, V. M., Mladetskyi, I. K., & Kuvaiev, M. V. (2020). Ulpa particle separation model in a spiral classifier. *Naukovyi Visnyk Natsionalnoho Hirnychoho Universytetu,* (1), 31-35. https://doi.org/10.33271/nvngu/2020-1/031.
14. Baziz, A., Bouzidi, N., & Eliche-Quesada, D. (2021). Recycling of gold mining reject from Amesmessa mine as ceramic raw material: microstructure and mechanical properties. *Environmental Science and Pollution Research, 28*, 46738-46747. https://doi.org/10.1007/s11356-020-12017-y.
15. Deniel, S., Tessier-Doyen, N., Dublanche-Tixier, C., Chateigner, D., & Blanchart, P. (2010). Transformation et caractérisation de céramiques mullite texturées à partir de phyllosilicates. *Journal of the European Ceramic Society, 30*, 2427-2434. https://doi.org/10.1016/j.jeurceramsoc.2010.04.029.
16. Montoya, N., Serrano, F. J., Reventós, M. M., Amigo, J. M., & Alarcón, J. (2010). Effet du TiO_2 sur la formation de mullite et les propriétés mécaniques de la porcelaine alumine. *Journal of the European Ceramic Society, 30*, 839-846. https://doi.org/10.1016/j.jeurceramsoc.2009.10.009.
17. Dana, K., & Das, S. K. (2004). Evolution of microstructure in flyash-containing porcelain body on heating at different temperatures. *Bulletin of Materials Science, 27*, 183-188. https://doi.org/10.1007/BF02708503.
18. Purohit, A., Chander, S., Hameed, A., Singh, P., & Dhaka, M. S. (2016). Structural, dielectric and surface morphological properties of ball clay with wet grinding for ceramic electrical insulators. *Materials Chemistry and Physics, 181*, 359-366. https://doi.org/10.1016/j.matchemphys.2016.06.070.
19. Savchuk, G. K., Petrochenko, T. P., & Klimza, A. A. (2013). Preparation and dielectric properties of celsian ceramics based on hexagonal $BaAl_2Si_2O_8$. *Inorganic Materials, 49*, 632-637. https://doi.org/10.1134/S0020168513060101.
20. Al-Hilli, M. F., & Al-Rasoul, K. T. (2010). Influence of glass addition and sintering temperature on the structure, mechanical properties and dielectric strength of high-voltage insulators. *Materials & Design, 31*, 3885-3890. https://doi.org/10.1016/j.matdes.2010.02.048.
21. Deng, J., Sun, X., Liu, S., Liu, L., Yan, T., Fang, L., & Elouadi, B. (2016). Influence of interface point defect on the dielectric properties of Y doped $CaCu_3Ti_4O_{12}$ ceramics. *Journal of advanced dielectrics*, *6*(01), 1650009. https://doi.org/10.1142/S2010135X16500090.

Переробка хвостів збагачення баритової руди у фарфор: мікроструктура та діелектричні властивості

О. Джезаірі[*1], *А. Бузіді*[2], *Н. Бузіді*[1], *В. Аяден*[1], *А. Бенселгуб*[3]

1 – Лабораторія матеріаловедення та технології виробництва, Технологічний факультет, Університет Беджая, м. Беджая, Алжир
2 – Лабораторія електротехнічного машинобудування, Технологічний факультет, Університет Беджая, м. Беджая, Алжир
3 – Відділ навколишнього середовища, моделювання та зміни клімату, Науково-дослідний центр з охорони довкілля, м. Аннаба, Алжир
* Автор-кореспондент e-mail: omar.djezairi@univ-bejaia.dz

Мета. Вивчення діелектричних властивостей фарфору, отриманого із суміші піску, каоліну й польового шпату. Останній був частково замінений твердими відходами бариту (ТВБ).

Методика. Дослідження включає підготовку фарфору з використанням традиційних методів твердофазної реакції із застосуванням двох температур випалення (1200 і 1300 °С) і витримки протягом 3 годин. Тверді відходи бариту поступово добавляють до суміші в кількості 0, 10, 20 и 30 %мас., замінюючи вміст польового шпату. Проводять структурні та діелектричні діагностики для вивчення того, як заміщення ТВБ впливає на макроскопічні діелектричні властивості. Мікроструктурні спостереження виявляють різні кристалічні фази та мікропори, що впливають на властивості матеріалу. Після випалення за температури 1200 °С основні мінералогічні фази складають муліт, анортит і кварц. За температури 1300 °С наступає фаза польового шпату разом із фазами анортиту та кварцу. Виявляють технологічні характеристики створених зразків фарфору, включаючи дилатометричні властивості, об'ємну щільність і пористість.

Результати. Діелектрична діагностика, проведена в межах діапазону частоти 102–105 Герц, показує, що відносні значення діелектричної проникності збільшуються з 4,3 до 7,4 для зразків, що випалюються за температури 1200 °С, і з 5,1 до 9,9 для тих, що випалюються за температури 1300 °С, зокрема для зразків, що вміщують 10 %мас. ТВБ. Крім того, тангенс кута діелектричних втрат зменшується зі збільшенням температури випалення. Можна точно розрахувати макроскопічну діелектричну проникність фарфору, використовуючи правило змішування, що добре узгоджується з експериментальними результатами.

Наукова новизна. Оригінальним вкладом є використання 10 % мас. твердих відходів бариту з копальні Букаїд для ефективного створення екологічно чистих фарфорових ізоляторів. Дослідження демонструє потенціал ТВБ в якості часткової заміни, тим самим сприяючи екологічності у виробництві фарфорових ізоляторів.

Практична значимість. Результати даного дослідження мають практичне значення для керамічної промисловості та виробництва ізоляторів, що сприяє розумінню способів удосконалення діелектричних властивостей фарфору шляхом включення ТВБ. Цей підхід сприяє виробництву екологічно чистих ізоляторів.

Ключові слова: *хвости збагачення, копальня Букаїд, відходи бариту, мікроструктура, діелектричні властивості*

The manuscript was submitted 28.07.23.